Liquid Crystals
Publication details, including instructions for authors and subscription information:
http://www.informaworld.com/smpp/title~content=t713926090

Ferroelectric liquid crystal dopants with a chiral (*R,R*)-2,3-difluorooctyloxy side-chain: host dependence of the polarization power

Matthew P. Thompson[a]; Torsten Hegmann[a]; Michael D. Wand[b]; Robert P. Lemieux[a]
[a] Chemistry Department, Queen's University, Kingston, Ontario, K7L 3N6, Canada [b] Displaytech Inc, 2602 Clover Basin Drive, Longmont, CO 80503

To cite this Article Thompson, Matthew P. , Hegmann, Torsten , Wand, Michael D. and Lemieux, Robert P.(2007) 'Ferroelectric liquid crystal dopants with a chiral (*R,R*)-2,3-difluorooctyloxy side-chain: host dependence of the polarization power', Liquid Crystals, 34: 8, 987 — 994

To link to this Article: DOI: 10.1080/02678290701526752

URL: http://dx.doi.org/10.1080/02678290701526752

Liquid Crystals, Vol. 34, No. 8, August 2007, 987–994

Ferroelectric liquid crystal dopants with a chiral (*R*,*R*)-2,3-difluorooctyloxy side-chain: host dependence of the polarization power

MATTHEW P. THOMPSON†, TORSTEN HEGMANN*†, MICHAEL D. WAND‡
and ROBERT P. LEMIEUX**†

†Chemistry Department, Queen's University, Kingston, Ontario, K7L 3N6, Canada
‡Displaytech Inc, 2602 Clover Basin Drive, Longmont, CO 80503, USA

(*Received 17 May 2007; accepted 5 June 2007*)

The polarization powers δ_p of four chiral dopants with (*R*,*R*)-2,3-difluorooctyloxy side-chains were measured in four liquid crystal hosts with isotropic (I)–nematic (N)–smectic A (SmA)–smectic C (SmC) phase sequences. The four chiral dopants differ in terms of their core structures: 2-phenylpyridine (**MDW950**), biphenyl (**5**), 2-phenylpyrimidine (**6**) and 2-(3-nitrophenyl)pyrimidine (**7**). In each case, δ_p varies with the structure of the liquid crystal host, which is consistent with the behaviour of so-called Type II dopants that normally feature a chiral core structure. The δ_p(host) profile was found to depend on the degree of biaxiality of the dopant core structure, and on the degree of steric coupling between the chiral 2,3-difluorooctyloxy side-chain and the core. Conformational analyses at the B3LYP/6-31G* level suggest that the 2,3-difluorooctyloxy side-chain is conformationally more rigid than conventional chiral side-chains due to the added electrostatic repulsion of the two adjacent fluoro groups combined with the hyperconjugative 'gauche effect', and may therefore have a higher degree of biaxiality on the time average. This biaxial character should make the chiral side-chain more sensitive to variations in quadrupolar ordering imposed by the SmC phase of the liquid crystal host, and may therefore explain the dependence of δ_p on the host structure reported herein.

1. Introduction

Intermolecular interactions between a mesogenic host and non-mesogenic additive (dopant) play an important role in defining the physical properties of many liquid crystalline formulations. Recent studies have shown that the induction of macroscopic chiral properties such as the helical structure of a chiral nematic (N*) or smectic C (SmC*) phase, the electroclinic tilt of a chiral smectic A (SmA*) phase and the spontaneous electric polarization (P_S) of a SmC* phase in a surface-stabilized ferroelectric liquid crystal (SSFLC) state can be understood in terms of molecular recognition between a chiral dopant and an achiral liquid crystal host [1–3]. The design of chiral dopants based on principles of molecular recognition is of particular interest in the case of ferroelectric SmC* liquid crystals, which are used in high-resolution reflective liquid-crystal-on-silicon (LCOS) microdisplays [4], and hold significant potential in nonlinear optics [5], chiral sensing [6] and photonics applications [7–9].

Commercial FLC mixtures are normally formed by mixing a chiral dopant in an achiral SmC liquid crystal host mixture with low viscosity and broad temperature range. The performance characteristics of FLC devices, including electrooptical switching time, second order NLO susceptibility and photoswitching threshold, often depend on the magnitude of P_S induced by the chiral dopant. Hence, a key aspect of FLC materials research is to understand the relationship between the molecular structure of a chiral dopant and the magnitude of the spontaneous polarization it induces [2, 10–12]. Siemensmeyer and Stegemeyer showed that this structure–property relationship can be expressed in terms of the polarization power δ_p according to [13],

$$\delta_p = \left(\frac{dP_o(x_d)}{dx_d} \right)_{x_d \to 0} \qquad (1)$$

where x_d is the mole fraction of chiral dopant and P_o is

---

*Present address: Department of Chemistry, University of Manitoba: Winnipeg, Manitoba, R3T 2N2, Canada.
**Corresponding author. Email: lemieux@chem.queensu.ca.

Liquid Crystals
ISSN 0267-8292 print/ISSN 1366-5855 online © 2007 Taylor & Francis
http://www.tandf.co.uk/journals
DOI: 10.1080/02678290701526752

the polarization normalized for variations in tilt angle θ according to [14].

$$P_o = P_S / \sin\theta. \qquad (2)$$

At the molecular level, the origins of P_S can be understood in terms of the rotational order about the director **n** imposed on the chiral dopant by the achiral liquid crystal host, together with the asymmetric conformational energy profile of any polar functional group that is coupled to one or more stereogenic centre(s) (stereo-polar unit), which results in an orientational bias of molecular dipoles along the polar axis of the FLC. According to the Boulder model, the achiral SmC phase is considered to be a supramolecular host, and the rotational ordering of a guest molecule is modelled by a mean-field potential, which qualitatively behaves like a receptor or 'binding site'. This binding site is C_{2h} symmetric and has a zigzag shape corresponding to a preferred rotational state in which the aromatic core is more tilted than the paraffinic side-chains, as deduced previously from comparisons of steric and optical tilt angles derived from X-ray scattering measurements and polarized microscopic observations, respectively [15].

The vast majority of chiral dopants known to induce a ferroelectric SmC* phase have stereo-polar units located in one of the side-chains and, in general, the polarization power of these dopants is more or less invariant of the achiral host structure. These were classified by Stegemeyer as 'Type I' dopants (e.g. **1** in scheme 1) to distinguish them from dopants with stereo-polar units located in the rigid core (e.g. **2** in scheme 1), which were classified as 'Type II' [16, 17]. Stegemeyer was the first to show that the polarization power of a Type II dopant varies with the structure of the achiral host, which may be viewed as a manifestation of molecular recognition via core–core interactions with the host molecules that cannot be achieved with conventional Type I dopants due to the higher degree of conformational disorder among side-chains in the diffuse layer structure of the SmC phase.

Stegemeyer explained the Type II host effect based on an extension of a microscopic model by Urbanc and Zeks [18], which suggests that the spontaneous polarization induced by a Type II chiral dopant is influenced by steric interactions with the surrounding host molecules that affect the rotational distribution of the core transverse dipole moment $\mu_\perp$ with respect to the polar axis of the SmC* phase [16]. The spontaneous polarization is expressed as a function of $\mu_\perp$ by:

$$P_S = N_1 \mu_\perp \cos\psi_o \langle\cos\psi\rangle, \qquad (3)$$

where N_1 is the dopant number density, ψ_o is the angle between $\mu_\perp$ and a molecular reference axis R of the dopant and <cos ψ> is the polar order parameter, which is related to the conformational asymmetry of the stereo-polar unit (figure 1). According to this model, which neglects quadrupolar ordering, the Type II host effect arises from variations in the rotational distribution of $\mu_\perp$caused by rigid core-core interactions with

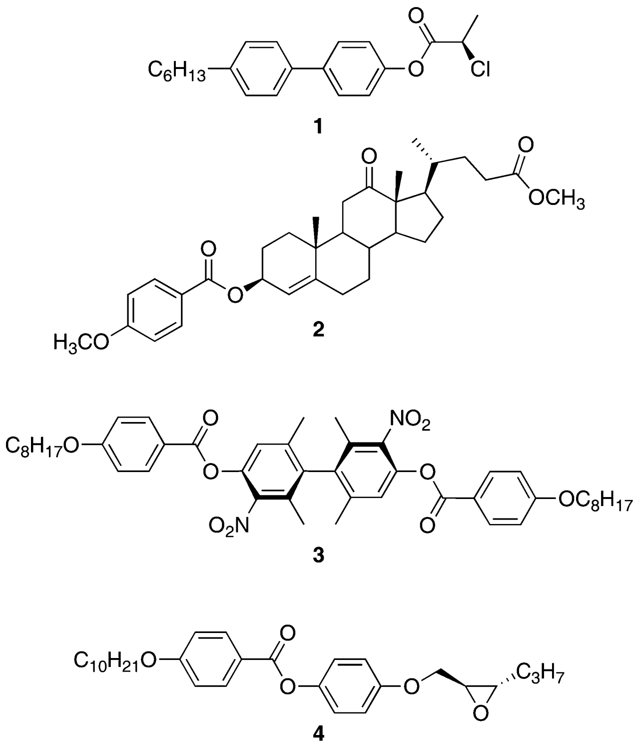

Scheme 1. Chemical structures of compounds **1**–**4**.

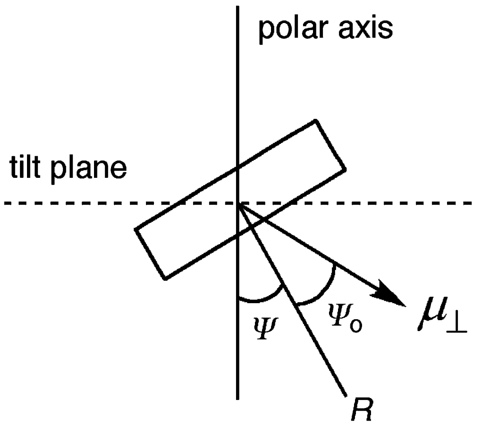

Figure 1. Schematic view of a Type II core along the director **n**, showing the orientation of the molecular reference axis R and the transverse dipole moment $\mu_\perp$ with respect to the polar axis and the tilt plane of the SmC* phase.

surrounding host molecules. Hence, a chiral dopant with high polar order may yet induce a low polarization in one host if $\mu_\perp$ is oriented near the tilt plane, and a high polarization in another host if $\mu_\perp$ is oriented near the polar axis. This model is consistent with the Boulder model, and the assumption that a chiral dopant plays the role of a 'passive' guest which adopts a conformation and rotational distribution that best fits the shape of the binding site. In another microscopic model, Stegemeyer suggested that intermolecular chirality transfer could contribute to the Type II host effect by causing a polar ordering of the host, thus inducing an additional polarization that scales with the transverse dipole moment of the host molecule [16]. In this case, the chiral dopant would be considered an 'active' guest perturbing its environment. More recently, we reported that Type II dopants with axially chiral biphenyl cores (e.g. **3** in scheme 1) exhibit remarkably high polarization powers in achiral liquid crystal hosts with complementary phenylpyrimidine cores, and that chiral perturbations exerted by these active guests on the liquid crystal host have a feedback effect that enhances δ_p [19, 20].

Stegemeyer noted that Type I behaviour normally holds for dopants with 'simple' stereo-polar units consisting of a single stereogenic centre in an aliphatic side-chain. Some chiral dopants with side-chains featuring more extended stereo-polar units, such as the chiral oxirane **4**, have been found to exhibit Type II behaviour [16]. These results were taken as evidence that the polar ordering of a chiral dopant is coupled to the quadrupolar ordering of its biaxial core in the SmC* phase if the stereo-polar unit is located within the core segment [17]. In the case of dopant **4** (scheme 1), the biaxial oxirane unit forms an extension of the biaxial phenyl benzoate core, and variations in the quadrupolar order parameter, which depends on short-range steric and dispersive core–core interactions, should therefore affect the magnitude of δ_p. In this paper, we report on the Type II behaviour of the Displaytech dopant **MDW950** (scheme 2), which also features an extended stereo-polar unit in the side-chain, and of the structural analogues **5**–**7** (scheme 2) with different core structures. Dopants with chiral 2,3-difluoroalkoxy side-chains are known to exhibit relatively large polarization powers with no adverse effect on the rotational viscosity of FLC mixtures, thus making them very attractive for use in SSFLC display applications [21]. However, all δ_p measurements reported for such dopants have been carried out in a single LC host consisting of a mixture of phenylpyrimidine derivatives, and no evidence of host dependence has therefore been reported.

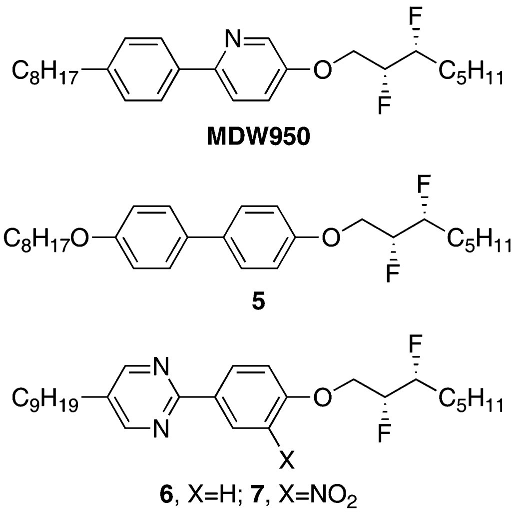

Scheme 2. Chemical structures of **MDW950** and compounds **5**–**7**.

2. Results and discussion

2.1. *Synthesis and mixture formulation*

The dopant **MDW950** was provided by Displaytech, Inc (Longmont, CO). The dopant **5** was obtained by sequential alkylation of 4,4′-biphenol (**8**) with 1-bromooctane and then with (*R,R*)-2,3-difluorooctyl tosylate, as shown in scheme 3. The dopants **6** and **7** were derived from the mesogen **10** (Clariant) via cleavage of the octyloxy side-chain with HBr, and then alkylation of **11** with (*R,R*)-2,3-difluorooctyl tosylate to give **6**. Nitration of the latter under standard conditions gave **7**.

None of the four dopants is liquid crystalline, but the unsubstituted dopants **MDW950**, **5** and **6** showed excellent miscibility with the four LC hosts used in this study (figure 2), up to mole fractions x_d of 0.20–0.25. For example, the phase diagram for mixtures of dopant **6** in **PhP** shows that adding the unsubstituted dopant causes only small decreases in phase transition temperatures, and a large increase in the temperature range of the SmC* phase (figure 3a). On the other hand, the nitro-substituted derivative **7** has a pronounced destabilizing effect in all four LC hosts, as shown in figure 3b for mixtures of **7** in **PhP**; in **DFT**, the SmC* phase is destabilized to such an extent that it vanishes at $x_\mathrm{d} \geqslant 0.10$.

2.2. *Polarization power measurements*

Homogeneous mixtures of the chiral dopants in the four LC hosts were aligned as SSFLC films using commercial ITO glass cells with rubbed polyimide surfaces and a cell gap of $4 \pm 0.5\,\mu\mathrm{m}$ (E.H.C. Co). Spontaneous

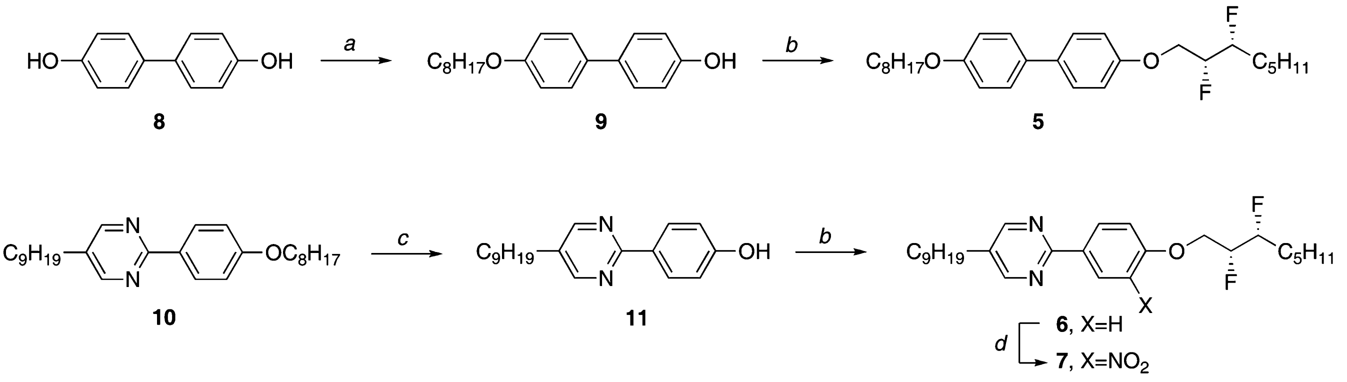

Scheme 3. Reagents and conditions: (a) Cs_2CO_3, 1-bromooctane, DMF, 89% yield; (b) (*R*,*R*)-2,3-difluorooctyl tosylate, Cs_2CO_3, DMF, 60% yield; (c) HBr, AcOH, 98% yield; (d) HNO_3, AcOH, 82% yield.

polarizations P_S and tilt angles θ were measured in the SmC* phase at 5 K below the SmA*–SmC* transition temperature ($T - T_C = -5\,K$) by the triangular wave method [22]. The corresponding P_o values were calculated using equation (2) and plotted as a function of x_d. All $P_o(x_d)$ plots gave good least-squares fits from which δ_p values were obtained. As shown in figure 4 and table 1, the sign of polarization induced by **MDW950** and **5**–**7** is negative in all four LC hosts, which is consistent with previous reports of chiral dopants with (*R*,*R*)-2,3-difluoroalkoxy side-chains [21]. The data also show that, in each case, δ_p varies significantly with the structure of the LC host.

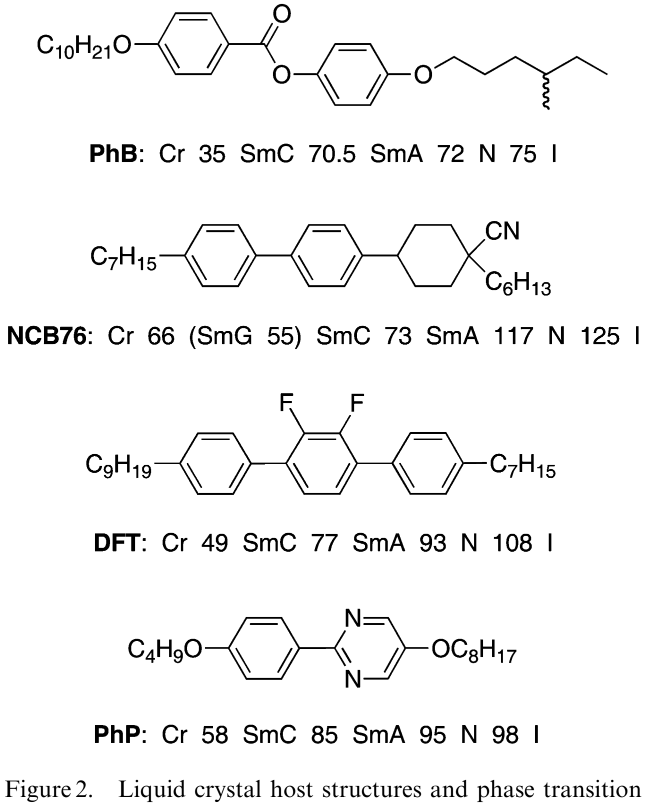

Figure 2. Liquid crystal host structures and phase transition temperatures (in °C).

As shown in figure 4a, the dependence of δ_p on the structure of the host follows roughly the same trend for the three dopants with unsubstituted cores, with the highest δ_p values obtained in the host **PhP** (ranging from -410 to $-435\,nC\,cm^{-2}$) and the lowest δ_p values obtained in the host **NCB76** (ranging from -115 to $-192\,nC\,cm^{-2}$). This is consistent with the reasonable assumption that polar ordering and rotational distribution of $\mu_\perp$ should not vary significantly with the dopant core structure, provided that steric coupling of the chiral side-chain to the core remains the same. Nevertheless, a distinction can be drawn between the δ_p(host) profile of dopant **6**, which features a planar 2-phenylpyrimidine core with maximum biaxiality, and those of dopants **MDW950** and **5**, which feature non-planar 2-phenylpyridine and biphenyl cores with lower biaxialities. The greater variance in δ_p observed with dopant **6** suggests that quadrupolar ordering may be more sensitive to differences in core-core interactions in this case due to the higher biaxiality of the phenylpyrimidine core.

The introduction of a nitro group *ortho* to the chiral 2,3-difluorooctyloxy side-chain (i.e. **7**) has a significant effect on the δ_p(host) profile. As shown in figure 4b, the most pronounced effect on δ_p was observed in the hosts **PhP** and **NCB76**. In **PhP**, the polarization power decreases in absolute value from $-442\,nC\,cm^{-2}$ to $-262\,nC\,cm^{-2}$ upon nitration of the phenylpyrimidine core of dopant **6**; in **NCB76**, the polarization power increases in absolute value from $-117\,nC\,cm^{-2}$ to $-361\,nC\,cm^{-2}$. The presence of the *ortho*-nitro substituent is expected to increase steric coupling between the chiral side-chain and the core, thus making the 2,3-difluorooctyloxy unit a more integral part of the dopant core structure. Such coupling between the core and the chiral side-chain is likely to affect the rotational

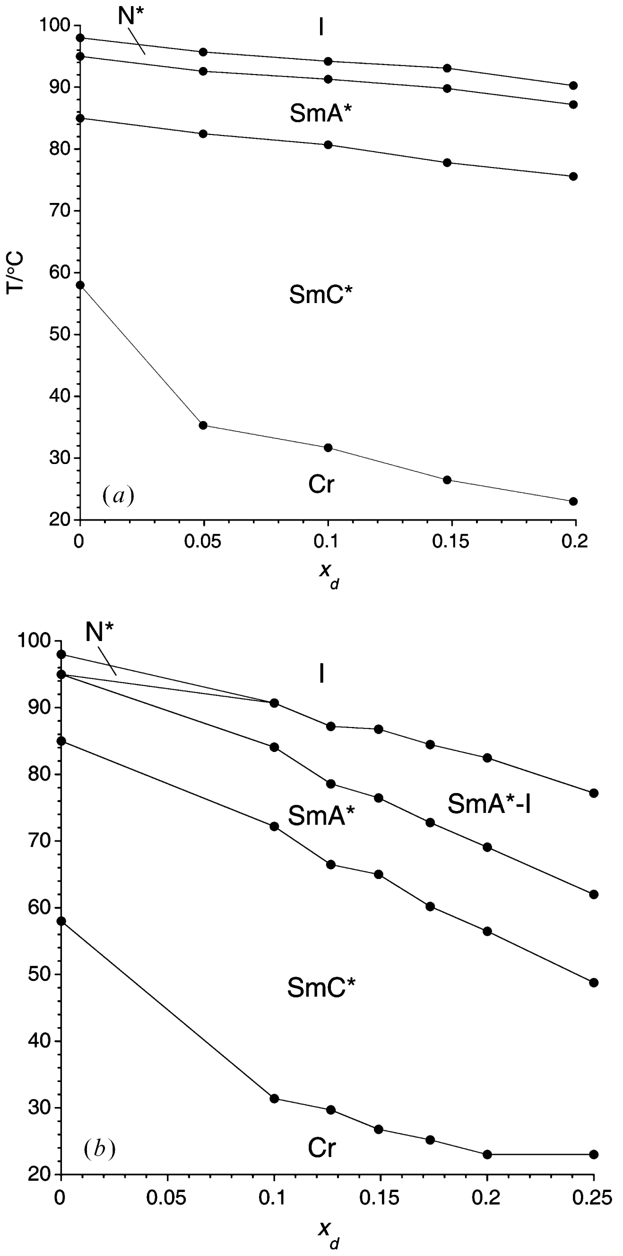

Figure 3. Phase diagrams for mixtures of (a) dopant **6** in **PhP** and (b) dopant **7** in **PhP**. Phase transition temperatures were measured by polarized optical microscopy on cooling.

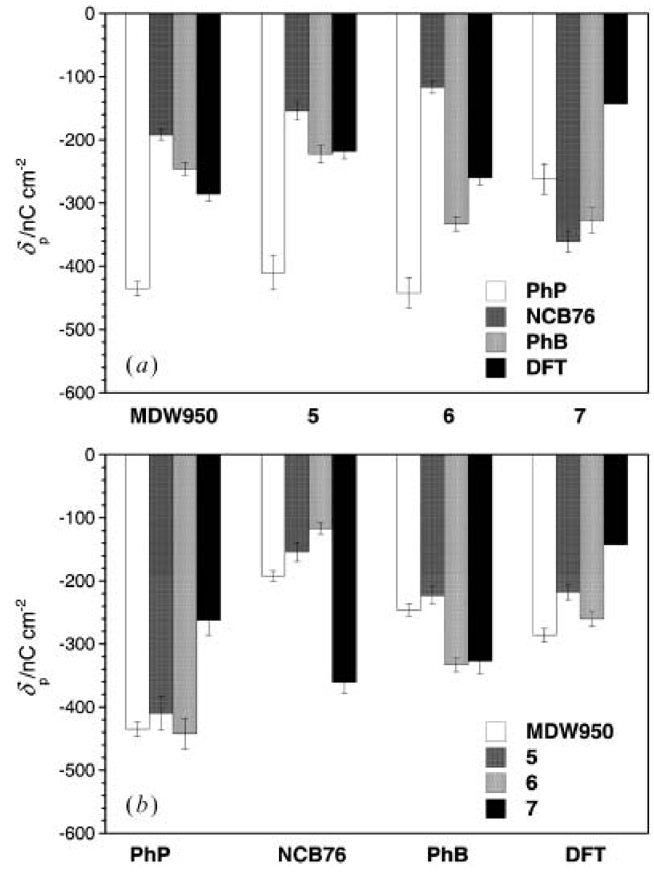

Figure 4. Bar graphs showing (a) a comparison of polarization power values for each dopant in the four different hosts and (b) a comparison of polarization power values for the four dopants in each host. Measurements were carried out at $T-T_C=-5$ K; the δ_p value for dopant **7** in **DFT** is based on a single measurement at x_d=0.05 due to poor miscibility in that host.

distribution of $\mu_\perp$ and/or the quadrupolar ordering of the dopant, which would account for the difference in δ_p(host) profiles.

2.3. *Conformational analyses*

The host dependence of δ_p observed with dopants featuring a chiral 2,3-difluorooctyloxy side-chain suggests that the structural unit formed by the two adjacent stereogenic centres has some degree of biaxiality, and may therefore be sensitive to changes in quadrupolar ordering in the SmC phase of a LC host. The biaxial character of the 2,3-difluorooctyloxy unit may arise from a greater conformational rigidity about the C-2–C-3 bond axis due to the repulsive interaction of the two fluoro groups and the 'gauche effect' associated with this structural unit [23, 24]. To test this hypothesis, we calculated conformational energy profiles at the B3LYP/6-31G* level for rotation about the C-2–C-3 bond axis in the model compounds **12a** and **12b** (scheme 4). The two conformational energy profiles (figure 5), which show relative energy as a function of the dihedral angle described by C-1, C-2, C-3 and C-4, are fairly similar except for the higher energy barrier between conformers I and II of the 2,3-difluoroalkoxy side-chain. This increase in energy barrier is due to the added electrostatic repulsion between the two eclipsed fluoro groups in the corresponding transition structure.

Table 1. Polarization powers δ_p of **MDW950**, **5**, **6**, and **7** in the hosts **PhP**, **NCB76**, **PhB** and **DFT** at $T - T_C = -5$ K.

	δ_p/nC cm^{-2} [a,b]			
Dopant	**PhP**	**NCB76**	**PhB**	**DFT**
MDW950	435 ± 11 (–)	192 ± 8 (–)	246 ± 10 (–)	286 ± 11 (–)
5	410 ± 27 (–)	154 ± 15 (–)	223 ± 14 (–)	218 ± 12 (–)
6	442 ± 24 (–)	117 ± 9 (–)	333 ± 11 (–)	260 ± 12 (–)
7	262 ± 24 (–)	361 ± 17 (–)	327 ± 20 (–)	143 (–)[c]

[a]Sign of polarization in parentheses. [b]Uncertainty is ± standard error of least-squares fit. [c]Based on a single measurement at $x_d = 0.05$ due to poor miscibility in that host.

The repulsive interaction between fluoro groups may also be responsible for the destabilization of conformer I relative to conformer III. Neither of these conformers benefits from hyperconjugative interactions between vicinal C–H and C–F bonds, the so-called 'gauche effect', which are present in conformer II, and shown to stabilize the *gauche* conformer of 1,2-difluoroethane [24]. The resulting increase in conformational rigidity of the 2,3-difluoroalkoxy side-chain relative to the 2-fluoroalkoxy side-chain, which is representative of conventional Type I dopants, imparts some degree of biaxiality that should make it more sensitive to variations in quadrupolar ordering imposed by the SmC phase of the LC host.

3. Summary

The polarization powers of four dopants with chiral 2,3-difluorooctyloxy side-chains and different biaryl core structures were measured in four LC hosts with isotropic–N–SmA–SmC phase sequences at $T - T_C = -5$ K. The results show that, in each case, δ_p varies with the structure of the LC host, which is consistent with the behaviour of a Type II dopant according to Stegemeyer *et al.* [16, 17]. The δ_p(host) profile was found to depend on the degree of biaxiality of the biaryl core structure, and on the degree of steric coupling between the chiral side-chain and the biaryl core. Conformational analyses at the B3LYP/6-31G* level suggest that a 2,3-difluorooctyloxy side-chain is conformationally more rigid than a monofluoro analogue due to the added electrostatic repulsion between the two adjacent fluoro groups combined with the hyperconjugative 'gauche effect', and may therefore have a higher degree of biaxiality on the time average. This biaxial character should make the 2,3-difluorooctyloxy stereo-polar unit more sensitive to variations in quadrupolar ordering imposed by the SmC phase of the LC host, and may therefore explain the dependence of δ_p observed with dopants featuring this chiral side-chain.

4. Experimental

4.1. *Synthesis*

4.1.1. (*R*,*R*)-4-(2,3-Difluorooctyloxy)-4'-octyloxy-1,1'-biphenyl (5). A solution of 4′-octyloxy-1,1′-biphenyl-4-ol (40 mg, 0.13 mmol), (*R*,*R*)-2,3-difluorooctyl tosylate (43 mg, 0.13 mmol) and Cs_2CO_3 (55 mg, 0.17mmol) in dry DMF (3 ml) was stirred at room temperature for 40 h. The reaction was diluted with H_2O and extracted with ether (3 × 15 ml). The combined organic extracts were washed with brine, dried ($MgSO_4$) and concentrated. Purification by flash chromatography on silical gel (9:1 hexanes:EtOAc) gave 40 mg (67%) of **5** as a white solid, m.p. 124–125°C. ^{1}H NMR (400 MHz, $CDCl_3$): δ 7.46 (m, 4H), 6.95 (m, 4H), 4.77 (m, 2H), 4.26 (m, 2H), 3.98 (t, 2H, J=8 Hz), 1.20–2.00 (m, 20H), 0.88 (m, 6H). ^{13}C NMR (100 MHz, $CDCl_3$): δ 13.9, 14.1, 22.4, 22.6, 24.6 (d, $J_{C\text{-}F}$=4 Hz), 26.1, 29.2, 29.3, 29.4, 30.1 (dd, $J_{C\text{-}F}$=4 Hz, 20 Hz), 31.4, 31.8, 66.5 (dd, $J_{C\text{-}F}$=7 Hz, 27 Hz), 68.1, 90.4 (dd, $J_{C\text{-}F}$=19 Hz, 47 Hz), 92.2 (dd, $J_{C\text{-}F}$=20 Hz, 42 Hz), 114.8, 127.7, 127.8, 133.0, 134.4, 157.2, 158.4. LRMS (CI) *m*/*z* 447 (100, M+H), 446 (60), 445 (23), 428 (17), 427 (75), 419 (26), 412 (10), 411 (44), 410 (23), 409 (15). HRMS (CI): calculated for $C_{28}H_{40}F_2O_2$, 447.3075; found, 447.3056.

4.1.2. (*R*,*R*)-2-(4-(2,3-Difluorooctyloxy)phenyl)-5-nonylpyrimidine (6). A solution of 4-(5-nonylpyrimidin-2-yl)phenol (60 mg, 0.2 mmol), (*R*,*R*)-2,3-difluorooctyl tosylate (64 mg, 0.2 mmol) and Cs_2CO_3 (131 mg, 0.4 mmol) in dry DMF (3 ml) was stirred at room temperature for 72 h. The reaction was diluted with H_2O and extracted with ether (3 × 15 ml). The combined organic extracts were washed with brine, dried ($MgSO_4$) and concentrated. Purification by flash chromatography on silica gel (9:1 hexanes:EtOAc) gave 68 mg (76%) of **6** as a white solid, m.p. 95–96°C. ^{1}H NMR (400 MHz, $CDCl_3$): δ 8.57 (s, 2H), 8.36 (d, 2H, J=8.4 Hz), 7.00 (d, 2H, J=8.4 Hz), 4.78 (m, 2H), 4.30 (m, 2H), 2.59 (t, 2H, J=7.5 Hz), 1.2–1.95 (m, 22H), 0.85–0.95 (m, 6H). ^{13}C NMR (100 MHz, $CDCl_3$): δ

13.9, 14.1, 22.4, 22.6, 24.6 (d, $J_{\text{C-F}}=5\,\text{Hz}$), 29.0, 29.2, 29.3, 29.5, 30.1 (dd, $J_{\text{C-F}}=5\,\text{Hz}$, 21 Hz), 30.2, 30.8, 31.4, 31.8, 66.4 ($J_{\text{C-F}}=7\,\text{Hz}$, 26 Hz), 90.3 (dd, $J_{\text{C-F}}=20\,\text{Hz}$, 50 Hz), 92.1 (dd, $J_{\text{C-F}}=20\,\text{Hz}$, 50 Hz), 114.5, 129.5, 131.1, 132.4, 157.0, 160.1, 162.9. LRMS (EI) *m/z* 446 (100, M^+), 444 (32), 347 (11), 334 (11), 333 (15), 185 (10). HRMS (EI): calculated for $C_{27}H_{40}F_2N_2O$, 446.3109; found, 446.3097.

4.1.3. (*R*,*R*)-2-(4-(2,3-Difluorooctyloxy)-3-nitrophenyl)-5-nonylpyrimidine (7).

A solution of **6** (68.5 mg, 0.15 mmol) in AcOH (5 ml) and HNO_3 (2.5 ml) was stirred for 10 min, then conc. H_2SO_4 (3 ml) was added and the solution was stirred at room temperature for 2 h. Concentrated H_2SO_4 (1.5 ml) was added again and the solution stirred for 10 min, then neutralized with aq. NaOH and extracted with ether (3 × 15 ml). The combined organic extracts were washed with brine, dried ($MgSO_4$) and concentrated. Recrystallization from hexanes gave 61 mg (82%) of **7** as a white solid, m.p. 89–90°C. ^{1}H NMR (400 MHz $CDCl_3$): δ 8.95 (s, 1H), 8.60–8.62 (m, 3H), 4.70–4.95 (m, 2H), 4.42–4.47 (m, 2H), 2.62 (t, 2H, $J=8\,\text{Hz}$), 1.20–2.00 (m, 24H), 0.85–0.92 (m, 6H). ^{13}C NMR (100 MHz $CDCl_3$): δ 13.9, 14.1, 22.4, 22.6, 24.6 (d, $J_{\text{C-F}}=5\,\text{Hz}$), 29.0, 29.2, 29.3, 29.4, 30.0 (dd, $J_{\text{C-F}}=5\,\text{Hz}$, 21 Hz), 30.2, 30.7, 31.4, 31.8, 67.7 (dd, $J_{\text{C-F}}=8\,\text{Hz}$, 28 Hz), 90.0 (dd, $J_{\text{C-F}}=20\,\text{Hz}$, 84 Hz), 91.7 (dd, $J_{\text{C-F}}=20\,\text{Hz}$, 80 Hz), 114.5, 125.4, 131.5, 133.2, 133.6, 140.2, 152.8, 157.1, 160.1. LRMS (EI), *m/z* 491 (100, M^+), 490 (11), 490 (44), 489 (13), 462 (29), 461 (23), 460 (42), 448 (18), 447 (18), 433 (10), 420 (59), 419 (41), 393 (16), 392 (16), 392 (62), 392 (42), 379 (63), 378 (43), 378 (13), 378 (12), 312 (40), 244 (52), 244 (42), 231 (30), 231 (29), 230 (59), 230 (45), 203 (18). HRMS (EI): calculated for $C_{27}H_{39}F_2N_3O_3$, 491.2959; found, 491.2959.

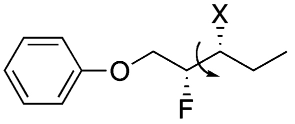

12a, X=F
12b, X=H

Scheme 4. Chemical structure of the model compounds **12a** and **12b**.

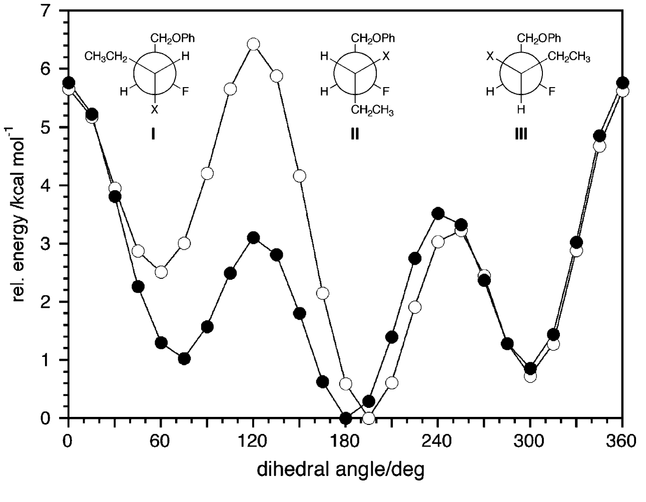

Figure 5. Relative conformational energy profiles for (*R*)-2,3-difluoropentyloxybenzene (**12a**, open circles) and (*S*)-2-fluoropentyloxybenzene (**12b**, filled circles) as a function of the dihedral angle defined by C-1, C-2, C-3 and C-4 according to B3LYP/6-31G* calculations.

4.2. *Ferroelectric polarization measurements*

Texture analyses and transition temperature measurements for the doped LC mixtures were performed using either a Nikon Labophot-2 POL or Nikon Eclipse E600 POL polarized microscope fitted with a Linkam LTS 350 hot stage. Spontaneous polarizations (P_S) were measured as a function of temperature by the triangular wave method (6 V μm^{-1}, 100 Hz) using a Displaytech APT-III polarization test bed in conjunction with the Linkam hot stage. Parallel rubbed polyimide-coated ITO glass cells (4 μm spacing) supplied by E.H.C. Co were used for the measurements [22]. Good alignment was obtained by slow cooling of the filled cells from the isotropic phase via the N* and SmA* phases (0.5–2 K min^{-1}). Tilt angles (θ) were measured as a function of temperature between crossed polarizers as half the rotation between two extinction positions corresponding to opposite polarization orientations. The sign of P_S along the polar axis was assigned from the relative configuration of the electrical field and the switching position of the sample according to the established convention [10].

Acknowledgments

We are grateful to the Natural Sciences and Engineering Research Council of Canada and the Canada Foundation for Innovation for support of this work. T.H. gratefully acknowledges the DAAD (German Academic Exchange Service) for a postdoctoral fellowship (Postdoc/NATO program, Grant D/01/28537).

References

[1] For reviews, see G.P. Spada, G. Proni. *Enantiomers*, **3**, 301 (1998); G. Solladié, R.G. Zimmermann. *Angew. Chem. Int. Ed.*, **23**, 348 (1984).

[2] R.P. Lemieux. *Accts Chem. Res.*, **34**, 845.

[3] T. Hegmann, M.R. Meadows, M.D. Wand, R.P. Lemieux. *J. Mater. Chem.*, **14**, 185.

[4] S.T. Lagerwall. *Ferroelectric and Antiferroelectric Liquid Crystals*, Wiley-VCH, Weinheim (1999); S.T. Lagerwall. In *Handbook of Liquid Crystals*, Vol. 2B, D. Demus, J.W. Goodby, G.W. Gray, H.-W. Spiess, V. Vill (Eds), Wiley-VCH, Weinheim (1998); D.M. Walba. *Science*, **270**, 250 (1995); N.A. Clark, S.T. Lagerwall. In *Ferroelectric Liquid Crystals: Principles, Properties and Applications*, J.W. Goodby, R. Blinc, N.A. Clark, S.T. Lagerwall, M.A. Osipov, S.A. Pikin, T. Sakurai, K. Yoshino, B. Zeks (Eds), Gordon & Breach, Philadelphia, PA (1991); J. Dijon. In *Liquid Crystals: Applications and Uses*, Vol. 1, B. Bahadur (Ed), World Scientific, Singapore (1990).

[5] D.M. Walba, L. Xiao, P. Keller, R. Shao, D. Link, N.A. Clark. *Pure appl. Chem.*, **71**, 2117 (1999); D.M. Walba, D.J. Dyer, T. Sierra, P.L. Cobben, R. Shao, N.A. Clark. *J. Am. chem. Soc.*, **118**, 1211 (1996); D.M. Walba, M.B. Ros, N.A. Clark, R. Shao, M.G. Robinson, J.Y. Liu, K.M. Johnson, D. Doroski. *J. Am. chem. Soc.*, **113**, 5471 (1991).

[6] D.M. Walba, D.J. Dyer, J.A. Rego, J. Niessink-Trotter, R. Shao, N.A. Clark. *Ferroelectrics*, **309**, 121.

[7] W.A. Crossland, T.D. Wilkinson. In *Handbook of Liquid Crystals,* Vol. 1, D. Demus, J.W. Goodby, G.W. Gray, H.-W. Spiess, V. Vill (Eds), Wiley-VCH, Weinheim.

[8] T. Ikeda, A. Kanazawa. In *Molecular Switches*, B.L. Feringa (Ed.), Wiley-VCH, Weinheim.

[9] R.P. Lemieux. *Soft Matter*, **1**, 348 (2005); R.P. Lemieux. *Chem. Rec.*, **3**, 288 (2004).

[10] D.M. Walba. In *Advances in the Synthesis and Reactivity of Solids,* Vol. 1, T.E. Mallouck (Eds), JAI Press, Greenwich, CT.

[11] M.A. Glaser. In *Advances in the Computer Simulations of Liquid Crystals*, C. Zannoni, P. Pasini (Eds), Kluwer, Dordrecht.

[12] J.W. Goodby. In *Ferroelectric Liquid Crystals: Principles, Properties and Applications*, J.W. Goodby, R. Blinc, N.A. Clark, S.T. Lagerwall, M.A. Osipov, S.A. Pikin, T. Sakurai, K. Yoshino, B.. Zeks (Eds), Gordon & Breach, Philadelphia, PA.

[13] K. Siemensmeyer, H. Stegemeyer. *Chem. Phys. Lett.*, **148**, 409.

[14] W. Kuczynski, H. Stegemeyer. *Chem. Phys. Lett.*, **70**, 123.

[15] R. Bartolino, J. Doucet, G. Durand. . Ann. Phys., **3**, 389.

[16] H. Stegemeyer, R. Meister, U. Hoffmann, A. Sprick, A. Becker. *J. Mater. Chem.*, **5**, 2183.

[17] M.A. Osipov, H. Stegemeyer, A. Sprick. *Phys. Rev. E*, **54**, 6387.

[18] B. Urbanc, B. Zeks. *Liq. Cryst.*, **5**, 1075.

[19] D. Vizitiu, C. Lazar, B.J. Halden, R.P. Lemieux. *J. Am. chem. Soc.*, **121**, 8229.

[20] C.S. Hartley, C. Lazar, M.D. Wand, R.P. Lemieux. *J. Am. chem. Soc.*, **124**, 13513.

[21] W.N. Thurmes, M.D. Wand, R.T. Vohra, K.M. More, D.M. Walba. *Liq. Cryst.*, **14**, 1061 (1993); M.D. Wand, R.T. Vohra, D.M. Walba, N.A. Clark, R. Shao. *Mol. Cryst. liq. Cryst.*, **202**, 183 (1991); W.N. Thurmes, M.D. Wand, R.T. Vohra, D.M. Walba. *Mol. Cryst. liq. Cryst.*, **204**, 1 (1991).

[22] K. Miyasato, S. Abe, H. Takezoe, A. Fukuda, E. Kuze. *Jap. J. appl. Phys.*, **22**, L661.

[23] S. Wolfe. *Accts Chem. Res.*, **5**, 102.

[24] L. Goodman, H. Gu, V. Pophristic. *J. phys. Chem. A*, **109**, 1223 (2005); and references therein.